

Intelligent Region-Based Steganography for High-Quality and Secure Medical Image Embedding

Kunkumalla Premchander¹, Dr. G. Soma Sekhar²

¹Research Scholar, Department of Computer Science, Mansarovar Global University, Sehore, Madhya Pradesh

²Supervisor, Department of Computer Science, Mansarovar Global University, Sehore, Madhya Pradesh

ABSTRACT

The growing adoption of digital medical imaging necessitates robust mechanisms for protecting sensitive patient information without compromising diagnostic quality. This paper proposes an intelligent region-based steganography method that integrates patient data within medical images while preserving visual fidelity. The approach leverages a Mask Region-Based Convolutional Neural Network (Mask-RCNN) to identify regions of minimal medical significance, ensuring that embedded information does not interfere with critical diagnostic areas. Data is concealed using discrete cosine transform (DCT)-based steganography, offering both security and high imperceptibility. The methodology encompasses three primary stages: neural network-based segmentation for region identification, DCT-based embedding of sensitive information, and extraction for accurate retrieval. Experiments conducted on the CHAOS dataset demonstrate the efficacy of the proposed method, achieving an average intersection over union (IoU) score of 0.9146, indicating precise segmentation. Evaluation metrics, including Peak Signal-to-Noise Ratio (PSNR) and embedding capacity analysis, reveal high-quality image preservation with minimal distortion and substantial data payload capability. Compared to existing techniques, the proposed method offers superior imperceptibility, secure data embedding, and efficient payload handling, making it a promising solution for confidential medical image management and secure healthcare data transmission.

Keywords: Steganography, Encryption, Security, Privacy, Medical-imaging

INTRODUCTION

Secret patient information must be kept safe in today's digital healthcare system. Ensuring the security and confidentiality of patient information saved and communicated with medical pictures is a major concern, especially as these images become more essential to diagnosis and treatment. Image data is generally not encrypted or otherwise protected during transmission or storage since traditional techniques of data security exist outside of the data itself. To solve this problem, researchers have offered a new framework that uses deep learning and signal processing to safely include private patient information into medical pictures without lowering the diagnostic quality of the images.

At its heart, this approach is novel because it can intelligently detect "insignificant regions" within medical images, or parts of the pictures that do not contain critical diagnostic data. A region-based convolutional neural network known for its high-precision picture segmentation capabilities, Mask-RCNN, is used to do this. The Mask-RCNN model is trained on labeled medical imaging datasets to differentiate between background regions that are less important and areas that are clinically relevant, such organs or abnormalities. Afterwards, data is embedded into these irrelevant portions, reducing the effect on the diagnostic value of the picture.

Discrete Cosine Transform (DCT) based steganography is used to embed patient data into the frequency domain of the picture after these locations have been found. By distributing the encoded data across many frequency components, DCT makes it more resilient and invisible to the naked eye. Due to the prevalence of compression and image processing assaults in medical imaging workflows, frequency domain embedding utilizing DCT offers superior protection compared to spatial domain approaches. With its two-pronged strategy—deep learning for area selection and DCT for safe embedding—this method provides an excellent compromise between privacy and picture fidelity.

There are essentially three distinct phases to the whole procedure. The first step in correctly segmenting the irrelevant areas is training the Mask-RCNN on datasets like CHAOS. Furthermore, these particular areas are used for DCT steganography to encode and embed sensitive patient data, such as identifying numbers or medical histories. Lastly, the embedded data is extracted during retrieval by using the reverse method, which preserves the picture quality. Multiple metrics are used to confirm that the system is performing as expected. Importantly, area segmentation has an average Intersection over Union (IoU) score of 0.9146, which indicates a high level of accuracy. In addition, Peak

Signal-to-Noise Ratio (PSNR) tests show that the stego pictures are very distortion-free and have excellent visual fidelity.

The experimental findings show that the system can handle large volumes of data undetectably, and they also show that it has a high embedding capacity and good payload management. Image quality and data security are two areas where our technology excels when compared to current steganographic and encryption methods. As a result, it's an encouraging step toward meeting data protection criteria for medical picture security while keeping clinical operations running smoothly.

REVIEW OF LITERATURE

Meng, Bowen & Yuan, Xiaochen et al., (2024) The smart healthcare system is a crucial part of modern healthcare since it improves medical treatment and allows for the exchange of electronic patient records (EPR). Nevertheless, a significant challenge remains in guaranteeing the confidentiality and authenticity of EPR data. We need to think outside the box and come up with solutions to this problem. Watermarking digital images is a common practice that guarantees the originality and integrity of digital images. It is very important to keep patients' medical imaging records private. We provide a hybrid strategy that combines encryption and watermarking to hide critical information in medical images. The suggested strategy for securing sensitive patient data is to use Advanced Encryption Standard-Galois/Counter Mode (AES-GCM) for first encryption and then embed the encrypted data. Using an intensity-based image segmentation method, the Region of Non-interest (RONI) is first chosen. This allows the encrypted patient information and the watermark to be integrated using a Fused Transform-Based method (FTBM). The study conducted in this paper used the comprehensive medical dataset called The Cancer Genome Atlas Lung Adenocarcinoma Collection (TCGA-LUAD). Medical image quality is maintained while patient data is securely protected using the proposed strategy, according to this research. When compared to the state-of-the-art approaches, the proposed one performs better in respect to security, integrity, and authenticity.

Yao, Ye & Wang, Ke et al., (2023) Recently, reversible data hiding in encrypted images (RDHEI) has attracted a lot of interest from researchers. In order to safely embed huge payloads into encrypted images, this research suggests a novel RDHEI method that, when coupled with bit-plane switching, block rearrangement, and sequential zero-valued high bit-planes compression, can be done. A record-breaking embedded payload is achieved by the proposed method, which is the first of its kind to block-wise compress globally zero-valued high bit-planes and adaptively distribute different Huffman indications based on the frequency of zero-valued bit-plane occurrences. By quietly clustering all embeddable bit-planes via bit-plane shifting and block rearrangement, most auxiliary information may be encrypted. The present RDHEI approaches employ unencrypted auxiliary information, which leads to poor security; this considerably increases security and makes data embedding and extraction much simpler. The experimental results demonstrate that the proposed technique exceeds previous state-of-the-art RDHEI methods in terms of payload and security. The average payload of BOWS-2, a dataset utilized by the public, is 3.705 bpp, whereas that of BOSS base is 3.793 bpp.

Gao, Guangyong & Tong, Shikun et al., (2021) Recent technical developments have made reversible data hiding (RDH) a popular topic in the data concealing research community. This research introduces the RDHACEM method, a synthetic contrast enhancement system that simultaneously improves image visual quality and increases embedding capacity. Medical photos employing state-of-the-art RDH methods are the main emphasis. The proposed method enhances picture quality by segmenting medical images into regions of interest (ROI) and non-ROI regions. It boosts image contrast and, by expanding the greyscale histogram of the ROI, enhances its embedding potential. Marked medical images generated by the proposed algorithm surpass those of state-of-the-art RDH methods when compared to these methods in terms of visual quality and ROI embedding capabilities.

Motomura, Ryota & Imaizumi et al., (2021) In this study, we provide a new method for reversible data hiding in encrypted images, which enables controllable hiding capacity and lossless compression efficiency. Two main objectives are to provide highly efficient lossless compression with a required concealing capacity and to enable the recovery of an embedded payload from a decrypted image. Even without data extraction, the proposed method can decrypt marked encrypted images and generate marked images. The original image is randomly divided into two halves. Two separate methods for reversible data hiding in encrypted pictures (RDH-EI) are used in our technique, one for each region. Consequently, in one place, you can do both post-processing lossless compression using image coding standards and decryption without extracting any data. In the other zone, the concealment rate is around 1 bpp, which is quite high. Experiments show that the proposed method is effective at lossless compression and has a hiding capacity.

PROPOSED METHOD

For high-capacity data concealing inside medical pictures, the suggested model innovatively blends the Mask-RCNN with the discrete cosine transform (DCT). Central to the model is Mask-RCNN, a cutting-edge deep learning framework renowned for its accuracy in instance segmentation jobs. By accurately locating and segmenting medically insignificant portions within pictures, this technique may be used to find possible places to implant safe data. For the

purpose of identifying areas where embedding may take place without impacting the diagnostic value of the picture, Mask-RCNN was selected because to its dual capacity to both categorize individual pixels in an image and accurately demarcate the borders of objects.

Following the identification of these zones, the model employs the discrete cosine transform (DCT), a fundamental method in signal processing for converting data from the spatial domain to the frequency domain. By focusing on the image's mid-frequency components, this transformation makes it easier to insert sensitive information into those parts. This is a calculated move, as these parts are less noticeable to the naked eye, making the embedding undetectable. To top it all off, DCT lets you tweak the embedding intensity, so you may compromise between capacity and quality of the images in a flexible way. To make sure that data is embedded in locations where it won't be recognized or impact picture quality, an adaptive selection system assesses the appropriateness of identified regions according to their complexity and texture. This further refines the embedding process. A major step forward in medical picture security has been achieved with this sophisticated method, which combines the segmentation power of Mask-RCNN with the embedding efficiency of DCT.

The main contribution of this work is the development of DICOM files that include patient information into medical pictures in a very subtle and unobtrusive way. The goal is to prevent misdiagnosis by using steganography principles. The method that has been developed entails hiding patient information in parts of the medical picture that don't really matter. In this context, "insignificant areas" are parts of a DICOM picture that do not include any vital medical information, such the black segments. Deep learning (DL) models efficiently extract unnecessary parts of the source pictures, making it easier to identify these areas. Afterwards, DCT-based steganography is used to covertly incorporate important medical information into these unnoticeable areas. Figure 1 is a schematic depicting the whole suggested procedure, including the three main steps of training the neural network, embedding it, and extracting its data.

Neural network training

Identifying small, unimportant regions in medical DICOM pictures and then using them to mask crucial data is the central idea of the suggested technique. We presuppose that accurately identifying the image's primary items is the gold standard for finding these areas. When compared to more conventional techniques, CNN-based approaches perform better when it comes to object recognition and segmentation inside pictures. Therefore, we use Mask-RCNN architecture²², which is known to be an effective method, particularly when it comes to medical image processing. The essential items that stand for the substantial area that has to be protected when data is embedded may be located with the help of this suggested design. Using the architecture shown in Figure 2, we train the Mask-RCNN model on several DICOM file datasets to yield binary segmentation masks. Two distinct phases make up this design:

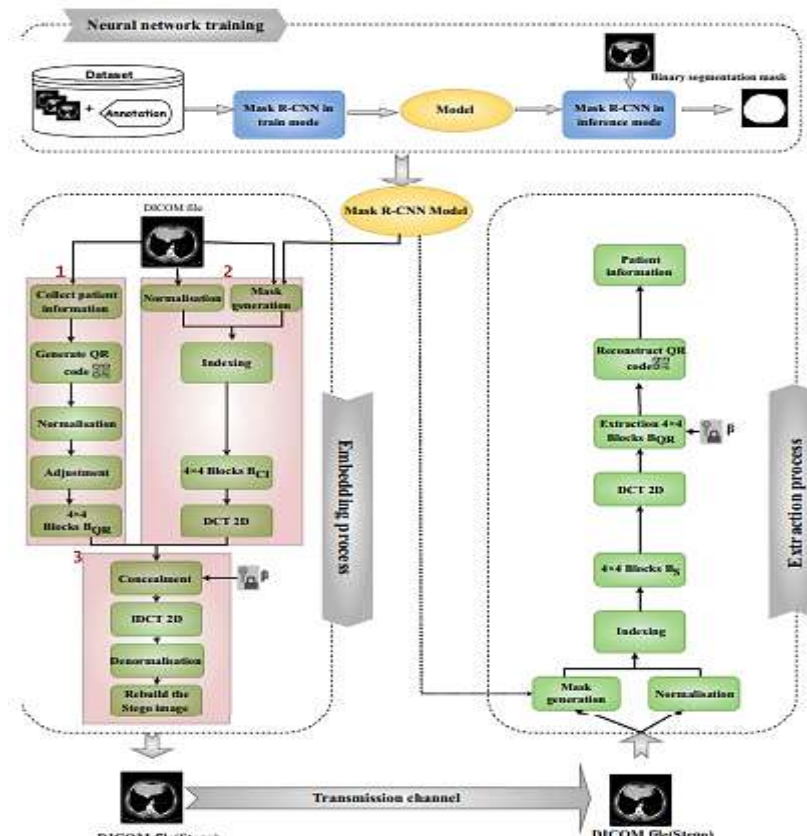


Figure 1: Detailed description of the steganography technique presented for consideration.

In the first phase, it processes a picture by creating a feature map and suggesting areas. A CNN backbone with ResNet and feature pyramid layers performs a number of operations on the input picture to produce the feature map. The feature map is sent into the region proposal network, which then generates areas that might hold objects.

Stage 2: RoIAlign, or the alignment of regions of interest, is what it's all about. Inputs include feature maps and region suggestions; outputs include object category, instance bounding-box, and binary segmentation masks for prediction, as well as areas of interest with fixed sizes derived from region proposals. To find the binary segmentation mask, this architecture is trained on different datasets. Pixels with a value of 1 indicate the object (the significant region) while pixels with a value of 0 represent the backdrop (the unimportant area). This model's loss function is defined by Eq (1).

$$L = L_{\text{class}} + L_{\text{box}} + L_{\text{mask}} \tag{1}$$

The classification loss is denoted as L_{class} , the bounding box regression loss as L_{box} , and the mask loss as L_{mask} .

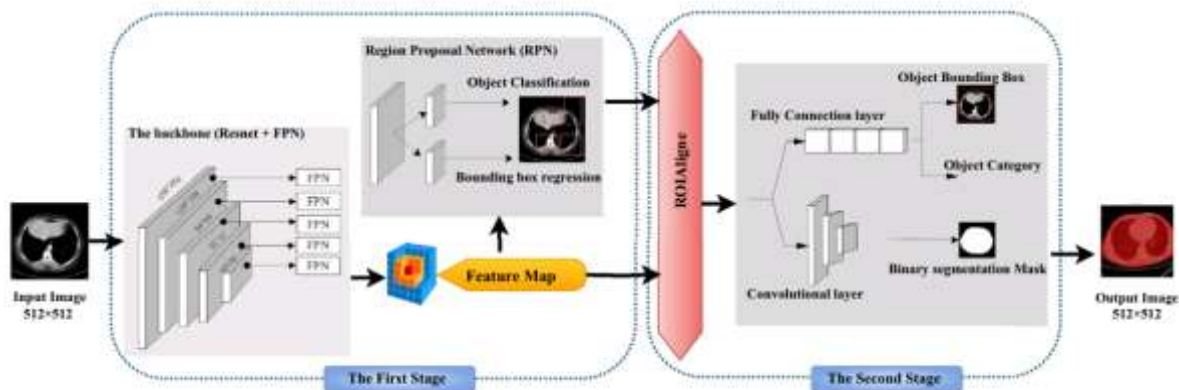


Figure 2: Hidden convolutional neural network design. Embedding process

In order to create a Stego picture, a sequence of sequential stages is used in the embedding process, which is also called the concealing process, to integrate sensitive patient data into DICOM images. To clarify, the previously determined unobtrusive region using the Mask-RCNN model is the center of this embedding. The three parts that make up this process are described in the sections that follow.

Sensitive information preprocessing

The first step is to use a QR Code generator to get the sensitive patient information out of the DICOM file and into a QR code picture. The Zxing library was used to produce QR codes that correspond to certain patient records; these codes are shown in Figure 3.

The values inside the generated QR code picture are then normalized to a range of 0 to 1 using Eq (2). Equation (3) is then used to fine-tune the normalized picture, with the experimentally-determined value of being set at $(\alpha = 0.02)$. The concealment step involves gradually hiding the four quadruple matrices, or blocks (B_{Qr}), that make up the corrected picture.

$$Norm(Img) = \frac{Img - Min(Img)}{\max(Img) - Min(Img)} \tag{2}$$

$$Adjustment(Msg) = \begin{cases} 1 - \alpha, Msg \geq 1 \\ \alpha, Msg = 0 \end{cases} \tag{3}$$

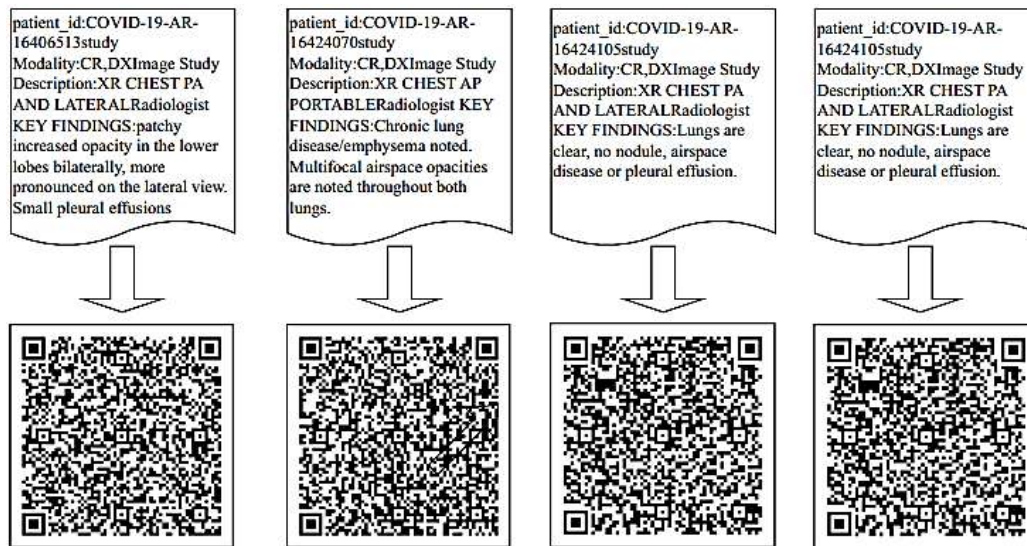


Figure 3: Visual representations of medical records shown with their corresponding QR codes.

Cover preprocessing

A two-stage preparation approach is used to the cover, which is obtained from the DICOM file. To start, a binary segmentation mask is produced by using the mask-RCNN model in inference mode to identify the irrelevant parts of the cover. Then, as DICOM pictures are usually 16-bit grayscale, we normalize the cover using Eq(2). such that its values fall on the [0, 1] interval.

In order to find the indices that correspond to the unimportant regions inside the normalized cover picture, also called the C_{ins} image, we use the mask that was created in the initial preprocessing phase. Afterwards, these inconsequential regions are subdivided into 4×4 blocks, abbreviated as (B_{Cins}) . Then, (B_{DCins}) blocks are generated by computing the transformation coefficients of (B_{Cins}) using the two-dimensional discrete cosine transform function (2D-DCT). By using the method given in Eq (4)., we may get the 2D-DCT for a matrix I (with dimensions $M \times N$).

$$C(u, v) = \alpha(u) \cdot \alpha(v) \times \left[\sum_{m=0}^{M-1} \sum_{n=0}^{N-1} I(m, n) \times \cos \frac{(2m+1)u\pi}{2M} \cos \frac{(2n+1)v\pi}{2N} \right] \begin{matrix} 0 \leq u \leq M-1 \\ 0 \leq v \leq N-1 \end{matrix} \quad (4)$$

Where

$$\alpha(u) = \begin{cases} 1 & 0 \leq u \leq M-1 \\ \sqrt{2} & 0 \leq v \leq N-1 \end{cases}$$

The position values and pixel values at position (m, n) in the spatial domain are represented by (m, n) and $I(m, n)$, respectively. At coordinates (u, v) in the domain of transformation, the appropriate position value and frequency coefficient are denoted as $C(u, v)$.

Information concealment

At this point, the four blocks that came from the cover (called (B_{DCins})) and the four blocks that represented the secret message (called (B_{QR})) that were created in the previous phase are combined. More precisely, (B_{QR}) is hidden inside (B_{DCins}) , so the corresponding block (B_s) in the Stego image is formed. The implementation of this hiding procedure is carried out by use of Eq (5).

$$B_s = IDCT2(Qun(B_{DCins}, B_{QR})) \quad (5)$$

Where

- B_s : Symbolizes the hidden portion of the Stego picture.
- Two-dimensional discrete cosine transform 2D-IDCT is the inverse of IDCT. Equation (6) describes this function.

$$I(m, n) = \alpha(u) \cdot \alpha(v) \times \left[\sum_{u=0}^{M-1} \sum_{v=0}^{N-1} C(u, v) \times \cos \frac{(2m+1)u\pi}{2M} \cos \frac{(2n+1)v\pi}{2N} \right] \quad (6)$$

Qun: Symbolizes the procedure that creates the pre-Stegoblock B_{SQ} by combining the B_{QR} and B_{DCins} blocks. The formula shown in Eq (7). is used to calculate this block.

$$B_{SQ}^{ij} = k + \left(\frac{4}{\beta} \times B_{QR}^{ij} \right) ; \quad \left(\frac{4k}{\beta} \right) < | B_{DCins}^{ij} | < \frac{(4k + 1)}{\beta} \quad (7)$$

Where:

- i, j : are respectively the i -th and j -th line and column in the block.
- β : is the number of intervals that satisfy the cover coefficients on the interval of $[0, 4]$.
- $k \in 1, 2, 3, \dots, \beta - 1$.

The final B_S that defines the Stego blocks is obtained by applying the inverse two-dimensional discrete cosine transform function (2D-IDCT) to B_{SQ} . Afterwards, the Stego blocks are combined to create the Stego picture, which is then de-normalized to limit values to the interval $[0, 65535]$. This essential step ensures that the Stego picture maintains the original encoding method and conforms to the 16-bit DICOM file format.

Input : Medical image with size $m \times n$, the QR code image of patient information
Output :Steganography medical image with size $m \times n$
1: Generate the binary segmentation mask
2: Normalize the cover
3: Normalize and adjust the QR code image
4: Get the index of 0 in the binary mask and generate the insignificant area of the Cover
5: Split the insignificant cover and the QR code into 4×4 blocks
6: Calculate the DCT transformation coefficients to cover insignificant block
7: Conceal the QR code block in the DCT coefficients with Equation.
8: Calculate the IDCT of the result blocks of step 7, to transform the image into the spatial domain
9: Reconstruct the Stego image

Algorithm 1: The embedding algorithm.

Extraction process

Recovering patient data concealed inside Stego pictures is the goal of the extraction procedure, which operates in opposite of the concealment process. Only users with the necessary key are permitted to do this retrieve. There are two separate steps to the extraction process: creating the mask and actually extracting the material.

While creating the mask, the Stego picture is fed into the inference mode of the Mask R-CNN model. A binary segmentation mask that is fine-tuned to identify irrelevant sections is produced by this process. An essential tool, this mask makes it easy to find and identify these spots—exactly where the hidden data is hiding.

Before beginning the extraction procedure, it is necessary to normalize the Stego picture such that all pixel values fall inside the interval $[0, 1]$. The location of the hidden pixels is deduced by using the binary mask of the Stego picture. The construction of the meaningless Stego matrix hinges on this decision. The matrix is then divided into 4×4 sections and moved into the frequency domain by using the Discrete Cosine Transform (DCT) function. A collection of transformation coefficients is the end result. These coefficients allow the extraction of the B_{QR} mini block, which corresponds to the QR code, by using the inverse merge operation (IQun). In its formal version, the extraction equation is given by Eq (8).

$$B_{QR} = IQun(DCT2(B_S)) \quad (8)$$

given by Eq (9)., which computes the inverse merging equation (IQun).

$$B_{QR} = (B_S - k) \times \beta/4; \quad \left(\frac{4k}{\beta} \right) < | B_S^{ij} | < \frac{(4k + 1)}{\beta} \quad (9)$$

The last step in creating the patient's QR code is to join the generated BQ blocks. In the other direction, Algorithm 2 encapsulates the procedure.

Input :Stego medical image with size $m \times n$

Output :Private patient information.

- 1: Generate the binary segmentation mask with size $m \times n$
- 2: Normalize the Stego
- 3: Get the index of 0 in the binary mask and generate the insignificant Stego area
- 4: Split the insignificant Stego into 4×4 blocks
- 5: Calculate the 2DCT transformation coefficients for Stego insignificant block using Eq.
- 6: Extract the QR code block from the DCT coefficients using the formula 9
- 7: Recreate the private patient information QR code

Algorithm 2: The extraction algorithm.

EXPERIMENTAL RESULTS

CHAOS dataset

The purpose of the CHAOS dataset is to use CT and MRI data to segment the liver, kidneys, and spleen, which are abdominal organs. Each of the two datasets corresponds to a different set of DICOM pictures. The first set includes computed tomography scans of 40 individuals who all have normal liver function. All of the datasets have the same patient orientation and alignment. The information is comprised of DICOM pictures that are 16 bits deep, have a 512×512 resolution, an x-y spacing of 0.7-0.8 mm, and an inter-slice distance (ISD) of 3-3.2 mm. Two separate MRI sequences, each scanning the abdomen with a unique mix of radiofrequency pulses and gradients, are housed in the second database, which contains 120 DICOM data sets. A 1.5 T Philips MRI is used to get the data sets, and it generates 12 bit DICOM pictures with a 256×256 resolution. There are 26–50 slices, x-y spacing ranges from 1.36–1.89 mm (average: 1.61 mm), and ISDs from 5.5–9 mm (average: 7.84 mm). One thousand two hundred DICOM pictures were chosen at random from the CHAOS collection. The photographs are separated into three categories: training, which uses 1023 images (11 patient images), validation, which uses 199 images (3 patient images), and testing, which uses 10 images. We used VIA Annotation Software to manually annotate these photos in the hopes of performing semantic segmentation to distinguish between the foreground, which we define as a Significant region, and the background, which we define as an obscure area.

Mask RCNN model training and evaluation

To create a Mask-RCNN model that can identify irrelevant regions in DICOM images, we used transfer learning. First, we adjusted the MS COCO model's pre-trained weights. This model is trained on a massive dataset for object identification and instance segmentation, consisting of 328k photos labelled with 91 different categories. Our detection aims were addressed by training the network on the CHAOS dataset with the MS COCO weights, following Matterport's suggested implementation of MASK-RCNN in 28. This allowed us to fine-tune the model.

Details of the setup used to train our form of the Mask-RCNN model are shown in Table 1. The backbone architecture, which is the ResNet101 architecture in this instance, is one of the parameters provided in the table. The number of photos used in each training iteration, known as the batch size, is set at 4. The classifying Feature Pyramid Network (FPN) makes use of a 1024-by-1024 completely linked layer. There is a learning rate of 0.001 and a momentum parameter of 0.9. Additionally, the weight decay value was adjusted to 0.0001 in order to avoid overfitting. One of the parameters utilized in training the region proposal network (RPN) is the RPN Train Anchors per Image, which is currently set at 256. along with a value of 4 for the Images Per GPU option, which means that each GPU can handle four images concurrently. The validation steps parameter is set to 50 and the steps per epoch value to 10. Training and validation iteration counts are controlled by these parameters.

Table 1. Setup of the mask R-CNN.

Parameter	Value
Backbone	resnet101
BATCH_SIZE	4
FPN_CLASSIF_FC_LAYERS_SIZE	1024
PU_COUNT	1
IMAGES_PER_GPU	4
LEARNING_MOMENTUM	0.9
LEARNING_RATE	0.001
RPN_TRAIN_ANCHORS_PER_IMAG	256
STEPS_PER_EPOCH	10
VALIDATION_STEPS	50
WEIGHT_DECAY	0.0001

The training was carried out on a computer with 16 GB of RAM, Intel UHD graphics, Core I7, and a 10th generation CPU. There are a total of 28 epochs used for training, with 8 dedicated to the head and 20 to fine-tuning all layers. Figure 4 shows the training and validation loss histograms. In figure, you can see the overall training and validation losses, and in you can see the losses associated with the MR-CNN mask. After training is complete, the MR-CNN general loss is 0.1291, and the MR-CNN mask loss is 0.0450.

Using the Intersection Over Union (IoU) metric²⁹, we assessed the degree to which the produced and annotated masks from the validation dataset overlapped. For the calculation of IoU, we use Eq (10):

$$(IOU) = \frac{\text{Area of intersection of two masks}}{\text{Area of Union of two masks}} \quad (10)$$

If the IoU is less than 1, it means the forecast is not accurate at all; otherwise, it means the prediction is insufficient. With an Average IoU of 0.9146, the model passed validation and is now safe to use.

Imperceptibility measurement

The embedded process that makes use of the trained MR-CNN model was the focus of the second phase of the experiment. Using ten photos, we validated the procedure. First, we used the embedding approach to get Stego pictures by hiding the QR codes (Message) in the Cover images after we extracted patient information from the DICOM files and converted it to QR codes. We continued by using the extraction procedure to decipher the Stego pictures for their hidden meanings.

Using Eq (12). We can also get the PSNR between two pictures in decibels:

$$MSE = \frac{\sum_{M,N} [I_1(m, n) - I_2(m, n)]^2}{M * N} \quad (11)$$

$$PSNR = 10 \log_{10} \left(\frac{R^2}{MSE} \right) \quad (12)$$

In this case, M and N denote the input photos' row and column counts, respectively. The input picture data type's maximum fluctuation is denoted by R. The PNSR typically ranges from 30 to 80 dB when dealing with 16-bit data.

Furthermore, we use NCC to assess the model's resilience and to evaluate the difference between the cover mask and the Stego mask; an NCC score close to 1 indicates that the two masks are comparable. Equation (13) provides the NCC formula.

$$NCC = \frac{\sum_{i=0}^m \sum_{j=0}^n (MC - \mu MC)(MS - \mu MS)}{\left(\sqrt{\sum_{i=0}^m (MC - \mu MC)^2} \right) \left(\sqrt{\sum_{i=0}^m (MS - \mu MS)^2} \right)} \quad (13)$$

In this case, μMC represents the average pixel value of the cover mask and μMS stands for the Stego mask.

The examined DICOM pictures' NCC and PSNR values, picture sizes, and scan types are all shown in Table 2. Our MR-CNN models are able to anticipate similar masks from the Cover and Stego pictures since all of the NCC values in the table are within the range of 0.83-1. This excellent forecast allows for the precise localization of the negligible region where covert actions occur.

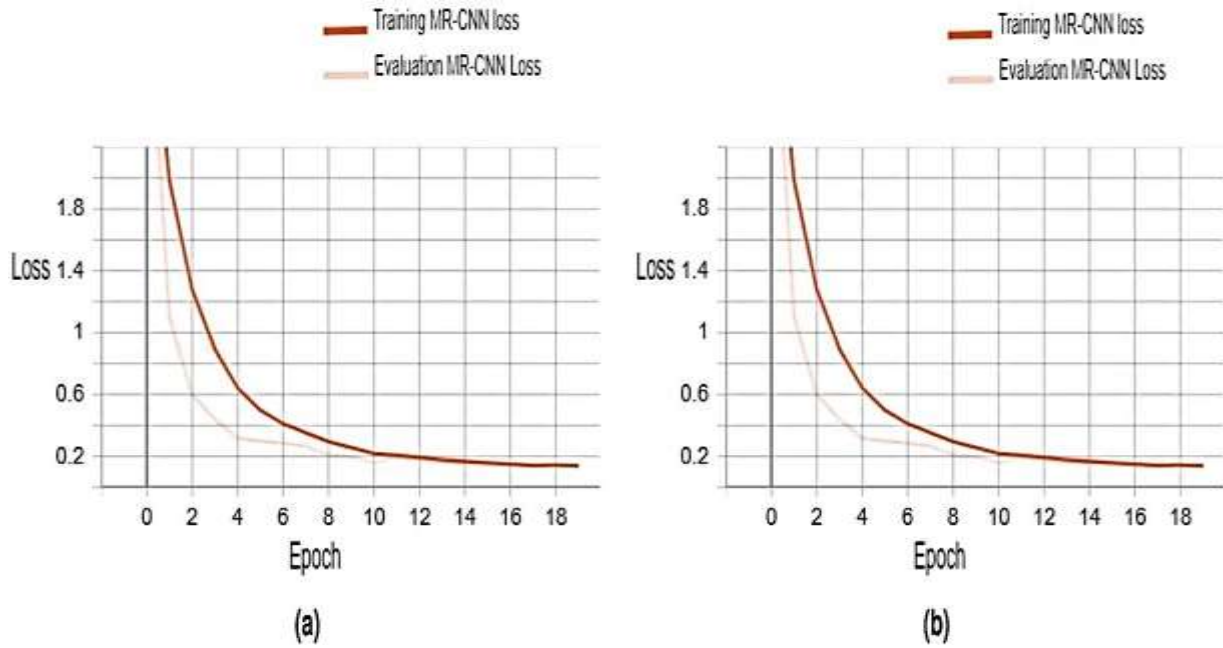


Figure 4: Setbacks in training and validating the model

Table 2: A measure of the test DICOM pictures' NCC and PSNR

Patient ID	1	2	3	4	5	6	7	8	9	10
Scan type	CT	CT	CT	CT	CT	M R	M R	M R	M R	M R
Image size (Pixel)	512 × 512	512 × 512	512 × 512	512 × 512	512 × 512	256 × 256	25 × 25 6	51 × 51 2	25 × 25 6	256 × 256
NCC	1.0 0	1.0 0	0.8 3	1.0 0	0.9 9	1.0 0	0.9 9	1.0 0	0.9 9	0.9 9
PSNR (dB)	116 .07	113 .69	115 .53	116 .57	116 .02	107 .47	11 0.3	11 7.4	11 0.3	110 .33

According to Table 2, the PNSR values range from 70.45 to 82.38 when the embedding parameters β are set to 1000 and 0.02 respectively. This suggests that our technique successfully hides critical patient information with a high degree of imperceptibility.

We assessed the PSNR by varying the embedding parameter β in order to investigate how the β coefficient impacts the final Stego quality. The resulting PSNR value is shown in Table 3.

Table 3: The mean squared errors (MSEs) for both the Cover and Stego DICOM datasets

Scan type	β										
	10	100	200	300	400	500	600	700	800	900	1000
CT											
1	75.05 1	95.955	102.01	105.55 7	108.09 4	110.03 9	111.57 8	112.99 3	114.12 9	115.22 5	116.07 4
2	72.66 1	93.551	99.64	103.16 6	105.72 9	107.66 1	109.22 2	110.61 8	111.74 8	112.88 8	113.69 5
3	74.55 5	95.424	72.483	101.50 0	105.02 9	107.56 3	109.49 4	112.45	113.58 5	114.69 6	115.53 2
4	75.13 6	96.313	102.44 2	105.99 8	108.55	110.51 7	112.07	113.44 4	114.64 4	115.72 3	116.57 1
5	75.07 6	95.914	101.99 4	105.52 6	108.06 7	109.99 5	111.55 7	112.94 5	114.07 6	115.19 1	116.02 2
Average	74.49 58	95.431 4	95.713 8	104.34 94	107.09 38	109.15 5	110.78 42	112.49	113.63 64	114.74 46	115.57 88
MRI											
1	66.49 4	87.347	93.425	96.949	99.500	101.44 7	102.98 4	104.39 4	105.53 3	106.64 3	107.47 3
2	69.38 9	90.217	96.281	99.803	102.34 5	104.28 3	105.82 3	107.22 7	108.36 5	109.47 6	110.30 4
3	76.47 2	97.313	103.38 5	106.90 4	109.44 7	111.38 6	112.92 5	114.32 1	115.47 2	116.58 1	117.40 0
4	69.38 9	90.217	96.281	99.803	102.34 5	104.28 3	105.82 3	107.22 7	108.36 5	109.47 6	110.30 4
5	69.39	90.222	96.29	99.816	102.36 2	104.30 3	105.84 7	107.25 3	108.39 3	109.50 5	110.33 3
Average	70.22 68	91.063 2	97.132 4	100.65 5	103.19 98	105.14 04	106.68 04	108.08 44	109.22 56	110.33 62	111.16 28

Cover and Stego DICOM pictures from 20 patients were compared for various b values, and the average results of the MSE values are shown in Table 3. A range of 2049.46 to 6152.98 was found for the average MSE values for $b = 500$. The highest value of b yields a high-quality Stego picture, since the lowest and highest MSE values were obtained for $b = 1000$ and $b = 100$, respectively. Table 4 displays the average PSNR values in decibels (dB) for comparisons between Stego and Cover pictures. For $b = 500$, the average PSNR values were 80.22 to 84.96 dB. The lowest PSNR value was 76.35 dB for patient 2 with $b = 100$, while the highest value was 85.39 dB for patient 14 with $b = 1000$. In most cases, a higher PSNR number indicates an invisible, high-quality signal.

CONCLUSION

A major step forward in protecting sensitive patient information and ensuring the safety of electronic health records has been made possible with the use of Mask-RCNN and DCT-based steganography to embed patient data into medical pictures. This solution successfully preserves diagnostic picture quality while protecting data using deep learning for intelligent area selection and frequency domain approaches for undetectable data embedding. To conceal sensitive information without affecting clinically relevant areas, Mask-RCNN accurately identifies non-critical regions in medical imaging. The approach becomes more resilient to compression and noise when combined with DCT-based steganography, which makes it a good fit for real-world medical imaging systems that rely on data integrity. The method's ability to preserve accuracy and visual quality is supported by experimental findings, such as a high IoU segmentation score and positive PSNR values. In comparison to conventional steganographic methods, our solution is more efficient and produces better results when it comes to securely retrieving embedded data. In conclusion, this approach offers a solid and workable way to protect sensitive patient information in medical photographs. It has the potential to make digital healthcare ecosystems safer and more secure by increasing privacy compliance in healthcare facilities, particularly in cases involving cloud storage, telemedicine, and picture transfer.

REFERENCES

- [1]. X. Li, W. Zhang, X. Gui, and B. Yang, "Efficient reversible data hiding based on multiple histograms modification," *IEEE Trans. Inf. Forensics Security*, vol. 10, no. 9, pp. 12-18, 2016.
- [2]. F. Huang, X. Qu, H. J. Kim, and J. Huang, "Reversible data hiding in JPEG images," *IEEE Trans. Circuits Syst. Video Technol.*, vol. 26, no. 9, pp. 1610-1621, Sep. 2016.

- [3]. Y.-Q. Shi, X. Li, X. Zhang, H.-T. Wu, and B. Ma, "Reversible data hiding: Advances in the past two decades," *IEEE Access*, vol. 4, no. 8, pp. 3210–3237, 2016.
- [4]. J. Zhou et al., "Secure reversible image data hiding over encrypted domain via key modulation," *IEEE Trans. Circuits Syst. Video Technol.*, vol. 26, no. 3, pp. 441–452, Mar. 2016.
- [5]. Z. Qian and X. Zhang, "Reversible data hiding in encrypted images with distributed source encoding," *IEEE Trans. Circuits Syst. Video Technol.*, vol. 26, no. 4, pp. 636–646, Apr. 2016.
- [6]. S. Zheng et al., "Lossless data hiding algorithm for encrypted images with high capacity," *Multimedia Tools Appl.*, vol. 75, no. 21, pp. 13765–13778, Nov. 2016.
- [7]. M. M. S. Rani and K. R. Euphrasia, "Dynamic hiding of message in RGB domain based on random channel indicator," *International Journal of Applied Engineering Research*, vol. 10, no. 76, pp. 478–483, 2015.
- [8]. F. Rashid, A. Miri, and I. Woungang, "Secure image deduplication through image compression," *Journal of Information Security and Applications*, vol. 20, no. 2, pp. 1–10, 2015.
- [9]. W. Zhang, X. Hu, X. Li, and N. Yu, "Optimal transition probability of reversible data hiding for general distortion metrics and its applications," *IEEE Trans. Image Process.*, vol. 24, no. 1, pp. 294–304, Jan. 2015.
- [10]. X. Liao and C. Shu, "Reversible data hiding in encrypted images based on absolute mean difference of multiple neighboring pixels," *J. Vis. Commun. Image Represent.*, vol. 28, no. 1, pp. 21–27, Apr. 2015.
- [11]. C. Qin and X. Zhang, "Effective reversible data hiding in encrypted image with privacy protection for image content," *J. Vis. Commun. Image Represent.*, vol. 31, no. 1, pp. 154–164, Aug. 2015.
- [12]. M. Li, D. Xiao, Y. Zhang, and H. Nan, "Reversible data hiding in encrypted images using cross division and additive homomorphism," *Signal Process. Image Commun.*, vol. 39, no. 2, pp. 234–248, Nov. 2015.
- [13]. X. Liao and C. Shu, "Reversible data hiding in encrypted images based on absolute mean difference of multiple neighbouring pixels," *J. Vis. Commun. Image Represent.*, vol. 28, no. 6, pp. 21–27, Apr. 2015.
- [14]. C. Qin and X. Zhang, "Effective reversible data hiding in encrypted image with privacy protection for image content," *J. Vis. Commun. Image Represent.*, vol. 31, no. 12, pp. 154–164, Aug. 2015.
- [15]. R. Motomura, S. Imaizumi, and H. Kiya, "A reversible data hiding method in encrypted images for controlling trade-off between hiding capacity and compression efficiency," *J. Imaging*, vol. 7, no. 12, p. 268, 2021.
- [16]. G. Gao, S. Tong, Z. Xia, B. Wu, L. Xu, and Z. Zhao, "Reversible data hiding with automatic contrast enhancement for medical images," *Signal Process.*, vol. 178, p. 107817, 2021.
- [17]. Y. Yao, K. Wang, Q. Chang, and S. Weng, "Reversible data hiding in encrypted images using global compression of zero-valued high bit-planes and block rearrangement," *IEEE Trans. Multimedia*, vol. 26, no. 1, pp. 1–14, 2023.
- [18]. Meng, X. Yuan, Q. Zhang, C. T. Lam, and G. Huang, "Encryption-then-embedding-based hybrid data hiding scheme for medical images," *J. King Saud Univ. Comput. Inf. Sci.*, vol. 36, no. 2458, p. 101932, 2024.